HIF-1 mediates adaptation to hypoxia by actively downregulating mitochondrial oxygen consumption

Ioanna Papandreou,[1,2] Rob A. Cairns,[1,2] Lucrezia Fontana,[1] Ai Lin Lim,[1] and Nicholas C. Denko[1,*]

[1] Division of Radiation and Cancer Biology, Department of Radiation Oncology, Stanford University School of Medicine, Stanford, California 94305
[2] These authors contributed equally to this work.
*Correspondence: ndenko@stanford.edu

Summary

The HIF-1 transcription factor drives hypoxic gene expression changes that are thought to be adaptive for cells exposed to a reduced-oxygen environment. For example, HIF-1 induces the expression of glycolytic genes. It is presumed that increased glycolysis is necessary to produce energy when low oxygen will not support oxidative phosphorylation at the mitochondria. However, we find that while HIF-1 stimulates glycolysis, it also actively represses mitochondrial function and oxygen consumption by inducing pyruvate dehydrogenase kinase 1 (PDK1). PDK1 phosphorylates and inhibits pyruvate dehydrogenase from using pyruvate to fuel the mitochondrial TCA cycle. This causes a drop in mitochondrial oxygen consumption and results in a relative increase in intracellular oxygen tension. We show by genetic means that HIF-1-dependent block to oxygen utilization results in increased oxygen availability, decreased cell death when total oxygen is limiting, and reduced cell death in response to the hypoxic cytotoxin tirapazamine.

Introduction

Tissue hypoxia results when supply of oxygen from the bloodstream does not meet demand from the cells in the tissue. Such a supply-demand mismatch can occur in physiologic conditions such as the exercising muscle, in the pathologic condition such as the ischemic heart, or in the tumor microenvironment (Hockel and Vaupel, 2001; Semenza, 2004). In either the physiologic circumstance or pathologic conditions, there is a molecular response from the cell in which a program of gene expression changes is initiated by the hypoxia-inducible factor-1 (HIF-1) transcription factor. This program of gene expression changes is thought to help the cells adapt to the stressful environment. For example, HIF-1-dependent expression of erythropoietin and angiogenic compounds results in increased blood vessel formation for delivery of a richer supply of oxygenated blood to the hypoxic tissue. Additionally, HIF-1 induction of glycolytic enzymes allows for production of energy when the mitochondria are starved of oxygen as a substrate for oxidative phosphorylation. We now find that this metabolic adaptation is more complex, with HIF-1 not only regulating the supply of oxygen from the bloodstream, but also actively regulating the oxygen demand of the tissue by reducing the activity of the major cellular consumer of oxygen, the mitochondria.

Perhaps the best-studied example of chronic hypoxia is the hypoxia associated with the tumor microenvironment (Brown and Giaccia, 1998). The tumor suffers from poor oxygen supply through a chaotic jumble of blood vessels that are unable to adequately perfuse the tumor cells. The oxygen tension within the tumor is also a function of the demand within the tissue, with oxygen consumption influencing the extent of tumor hypoxia (Gulledge and Dewhirst, 1996; Papandreou et al., 2005b). The net result is that a large fraction of the tumor cells are hypoxic. Oxygen tensions within the tumor range from near normal at the capillary wall, to near zero in the perinecrotic regions. This perfusion-limited hypoxia is a potent microenvironmental stress during tumor evolution (Graeber et al., 1996; Hockel and Vaupel, 2001) and an important variable capable of predicting for poor patient outcome. (Brizel et al., 1996; Cairns and Hill, 2004; Hockel et al., 1996; Nordsmark and Overgaard, 2004).

The HIF-1 transcription factor was first identified based on its ability to activate the erythropoetin gene in response to hypoxia (Wang and Semenza, 1993). Since then, it is has been shown to be activated by hypoxia in many cells and tissues, where it can induce hypoxia-responsive target genes such as VEGF and Glut1 (Airley et al., 2001; Kimura et al., 2004). The connection between HIF-regulation and human cancer was directly linked when it was discovered that the VHL tumor suppressor gene was part of the molecular complex responsible for the oxic degradation of HIF-1α (Maxwell et al., 1999). In normoxia, a family of prolyl hydroxylase enzymes uses molecular oxygen as a substrate and modifies HIF-1α and HIF2α by hydroxylation of prolines 564 and 402 (Bruick and McKnight, 2001; Epstein et al., 2001). VHL then recognizes the modified HIF-α proteins, acts as an E3-type of ubiquitin ligase, and along with elongins B and C is responsible for the polyubiquitination of HIF-αs and their proteosomal degradation (Bruick and McKnight, 2001; Chan et al., 2002; Ivan et al., 2001; Jaakkola et al., 2001). Mutations in VHL lead to constitutive HIF-1 gene expression, and predispose humans to cancer. The ability to recognize modified HIF-αs is at least partly responsible for VHL activity as a tumor suppressor, as introduction of nondegradable HIF-2α is capable of overcoming the growth–inhibitory activity of wild-type (wt) VHL in renal cancer cells (Kondo et al., 2003).

Mitochondrial function can be regulated by PDK1 expression. Mitochondrial oxidative phosphorylation (OXPHOS) is regulated by several mechanisms, including substrate availability (Brown, 1992). The major substrates for OXPHOS are oxygen, which is the terminal electron acceptor, and pyruvate, which is the primary carbon source. Pyruvate is the end product of glycolysis

and is converted to acetyl-CoA through the activity of the pyruvate dehydrogenase complex of enzymes. The acetyl-CoA then directly enters the TCA cycle at citrate synthase where it is combined with oxaloacetate to generate citrate. In metazoans, the conversion of pyruvate to acetyl-CoA is irreversible and therefore represents a critical regulatory point in cellular energy metabolism. Pyruvate dehydrogenase is regulated by three known mechanisms: it is inhibited by acetyl-CoA and NADH, it is stimulated by reduced energy in the cell, and it is inhibited by regulatory phosphorylation of its E1 subunit by pyruvate dehydrogenase kinase (PDK) (Holness and Sugden, 2003; Sugden and Holness, 2003). There are four members of the PDK family in vertebrates, each with specific tissue distributions (Roche et al., 2001). PDK expression has been observed in human tumor biopsies (Koukourakis et al., 2005), and we have reported that PDK3 is hypoxia-inducible in some cell types (Denko et al., 2003). In this manuscript, we find that PDK1 is also a hypoxia-responsive protein that actively regulates the function of the mitochondria under hypoxic conditions by reducing pyruvate entry into the TCA cycle. By excluding pyruvate from mitochondrial consumption, PDK1 induction may increase the conversion of pyruvate to lactate, which is in turn shunted to the extracellular space, regenerating NAD for continued glycolysis.

Results

Identification of HIF-dependent mitochondrial proteins through genomic and bioinformatics approaches

In order to help elucidate the role of HIF-1α in regulating metabolism, we undertook a genomic search for genes that were regulated by HIF-1 in tumor cells exposed to hypoxia in vitro. We used genetically matched human RCC4 cells that had lost VHL during tumorigenesis and displayed constitutive HIF-1 activity, and a cell line engineered to re-express VHL to establish hypoxia-dependent HIF activation. These cells were treated with 18 hr of stringent hypoxia (<0.01% oxygen), and microarray analysis performed. Using a strict 2.5-fold elevation as our cutoff, we identified 173 genes that were regulated by hypoxia and/or VHL status (Table S1 in the Supplemental Data available with this article online). We used the pattern of expression in these experiments to identify putative HIF-regulated genes—ones that were constitutively elevated in the parent RCC4s independent of hypoxia, downregulated in the RCC4VHL cells under normoxia, and elevated in response to hypoxia. Of the 173 hypoxia and VHL-regulated genes, 74 fit the putative HIF-1 target pattern. The open reading frames of these genes were run through a pair of bioinformatics engines in order to predict subcellular localization, and 10 proteins scored as mitochondrial on at least one engine. The genes, fold induction, and mitochondrial scores are listed in Table 1.

Table 1. Identification of putative HIF-1α-regulated mitochondrial proteins through microarray, bioinformatics, and data-mining approaches

Gene	Identifier	Ind 1	Ind 2	Loc 1	Loc 2
SLC9A6 Na/H exchanger 6	AF030409	13.0	19.0	M	Mit
GPT2 Glut/pyr transaminase	AY029173	10.0	10.0	M	C/Mit
MCG45806 (Rab 39-like)	Hs.55272	13.0	19.0	–	Mit
BNIP3 E1B 19 kD-interacting protein 3	AF002697	9.1	4.3	–	Mem Mit
PPP1R3C protein phosphatase 1 3C	BC012625	7.3	6.9	M	C
AP1G1 Adaptor-related complex 1 1	Y12226	3.5	3.2	M	C
PDK1 Pyruvate dehydrogenase kin 1	L42450	3.1	5.9	M	Mit
Hypothetical protein FLJ36666	AK093985	2.9	9.0	–	Mit
PFKFB4 phosphofructo-2 kinase 4	BC010269	2.6	2.6	–	Mit
PTPN14 Protein tyr phosphotase	BC017300	2.5	3.0	M	Mem Mit

Ind 1 and 2 represent the fold induction for the indicated gene based on the two microarray experiments, Loc1 is the predicted subcellular location based on TargetP V1.0 (www.cbs.dtu.dk), and Loc2 is the predicted subcellular localization based on ProtComp V6.0 (www.softberry.com).

HIF-1 downregulates mitochondrial oxygen consumption

Having identified several putative HIF-1 responsive gene products that had the potential to regulate mitochondrial function, we then directly measured mitochondrial oxygen consumption in cells exposed to long-term hypoxia. While other groups have studied mitochondrial function under acute hypoxia (Chandel et al., 1997), this is one of the first descriptions of mitochondrial function after long-term hypoxia where there have been extensive hypoxia-induced gene expression changes. Figure 1A is an example of the primary oxygen trace from a Clark electrode showing a drop in oxygen concentration in cell suspensions of primary fibroblasts taken from normoxic and hypoxic cultures. The slope of the curve is a direct measure of the total cellular oxygen consumption rate. Exposure of either primary human or immortalized mouse fibroblasts to 24 hr of hypoxia resulted in a reduction of this rate by approximately 50% (Figures 1A and 1B). In these experiments, the oxygen consumption can be stimulated with the mitochondrial uncoupling agent CCCP (carbonyl cyanide 3-chloro phenylhydrazone) and was completely inhibited by 2 mM potassium cyanide. We determined that the change in total cellular oxygen consumption was due to changes in mitochondrial activity by the use of the cell-permeable poison of mitochondrial complex 3, Antimycin A. Figure 1C shows that the difference in the normoxic and hypoxic oxygen consumption in murine fibroblasts is entirely due to the Antimycin-sensitive mitochondrial consumption. The kinetics with which mitochondrial function slows in hypoxic tumor cells also suggests that it is due to gene expression changes because it takes over 6 hr to achieve maximal reduction, and the reversal of this repression requires at least another 6 hr of reoxygenation (Figure 1D). These effects are not likely due to proliferation or toxicity of the treatments as these conditions are not growth inhibitory or toxic to the cells (Papandreou et al., 2005a).

Since we had predicted from the gene expression data that the mitochondrial oxygen consumption changes were due to HIF-1-mediated expression changes, we tested several genetically matched systems to determine what role HIF-1 played in the process (Figure 2). We first tested the cell lines that had been used for microarray analysis and found that the parental RCC4 cells had reduced mitochondrial oxygen consumption when compared to the VHL-reintroduced cells. Oxygen consumption in the parental cells was insensitive to hypoxia, while it was reduced by hypoxia in the wild-type VHL-transfected cell lines. Interestingly, stable introduction of a tumor-derived mutant VHL (Y98H) that cannot degrade HIF was also unable to restore oxygen consumption. These results indicate that increased expression of HIF-1 is sufficient to reduce oxygen consumption (Figure 2A). We also investigated whether HIF-1

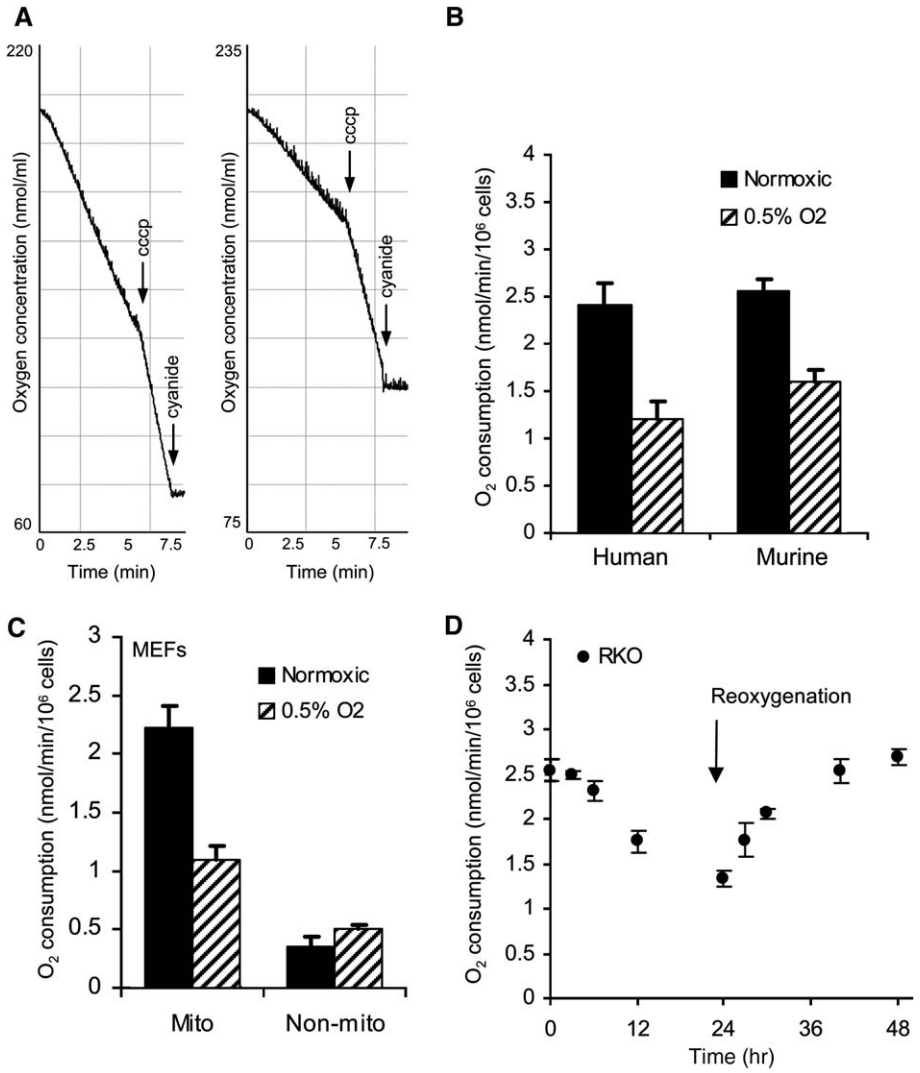

Figure 1. Hypoxia inhibits mitochondrial oxygen consumption

A) Oxygen concentration curves generated using a Clark electrode for fibroblast suspensions from cultures exposed to normoxia or hypoxia for 24 hr. Arrows indicate addition of the mitochondrial uncoupler CCCP and cytochrome poison cyanide. The slope of the curve is a measure of the rate of oxygen consumption.

B) Average oxygen consumption rates in normal human fibroblasts and immortalized murine fibroblasts cultured in normoxia or 0.5% O_2 for 24 hr.

C) Fraction of total oxygen consumption due to mitochondrial versus nonmitochondrial consumption in wild-type murine fibroblasts. Mitochondrial consumption was determined using 1ug/ml of the cell permeable complex 3 inhibitor Antimycin A.

D) Change in oxygen consumption in RKO cells after exposure to the indicated time in 0.5% O_2, and time to recovery in normoxia following 24 hr hypoxia.

For all graphs, the error bars represent the standard error of the mean.

induction was required for the observed reduction in oxygen consumption in hypoxia using two genetically matched systems. We measured normoxic and hypoxic oxygen consumption in murine fibroblasts derived from wild-type or HIF-1α null embryos (Figure 2B) and from human RKO tumor cells and RKO cells constitutively expressing ShRNAs directed against the HIF-1α gene (Figures 2C and 4C). Neither of the HIF-deficient cell systems was able to reduce oxygen consumption in response to hypoxia. These data from the HIF-overexpressing RCC cells and the HIF-deficient cells indicate that HIF-1 is both necessary and sufficient for reducing mitochondrial oxygen consumption in hypoxia.

HIF-dependent mitochondrial changes are functional, not structural

Because addition of CCCP could increase oxygen consumption even in the hypoxia-treated cells, we hypothesized that the hypoxic inhibition was a regulated activity, not a structural change in the mitochondria in response to hypoxic stress. We confirmed this interpretation by examining several additional mitochondrial characteristics in hypoxic cells such as mitochondrial morphology, quantity, and membrane potential. We examined morphology by visual inspection of both the transiently transfected mitochondrially localized DsRed protein and the endogenous mitochondrial protein cytochrome C. Both markers were indistinguishable in the parental RCC4 and the RCC4VHL cells (Figure 3A). Likewise, we measured the mitochondrial membrane potential with the functional dye rhodamine 123 and found that it was identical in the matched RCC4 cells and the matched HIF wt and knockout (KO) cells when cultured in normoxia or hypoxia (Figure 3B). Finally, we determined that the quantity of mitochondria per cell was not altered in response to HIF or hypoxia by showing that the amount of the mitochondrial marker protein HSP60 was identical in the RCC4 and HIF cell lines (Figure 3C)

PDK1 is a HIF-1 inducible target protein

After examination of the list of putative HIF-regulated mitochondrial target genes, we hypothesized that PDK1 could mediate the functional changes that we observed in hypoxia. We therefore investigated PDK1 protein expression in response to HIF and hypoxia in the genetically matched cell systems. Figure 4A shows that in the RCC4 cells PDK1 and the HIF-target gene BNip3 (Greijer et al., 2005; Papandreou et al., 2005a) were

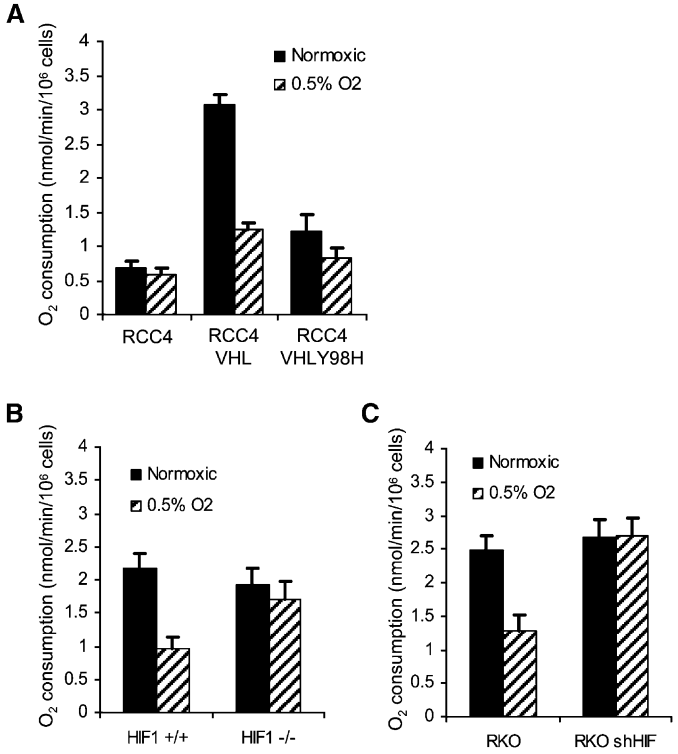

Figure 2. Hypoxic reduction in mitochondrial oxygen consumption is HIF-1 dependent

A) Average oxygen consumption rates in vhl-deficient RCC4 cells, RCC4/VHL cells, and RCC4/VHLY98H cells after exposure to 24 hr of normoxia or 0.5% O_2.
B) Average oxygen consumption rates in HIF wt and HIF KO murine fibroblasts after exposure to normoxia or 0.5% O_2 for 24 hr.
C) Average oxygen consumption rates in parental RKO cells and ShRNAHIF-1α RKO cells after exposure to 24 hr of normoxia or 0.5% O_2.
For all graphs, the error bars represent the standard error of the mean.

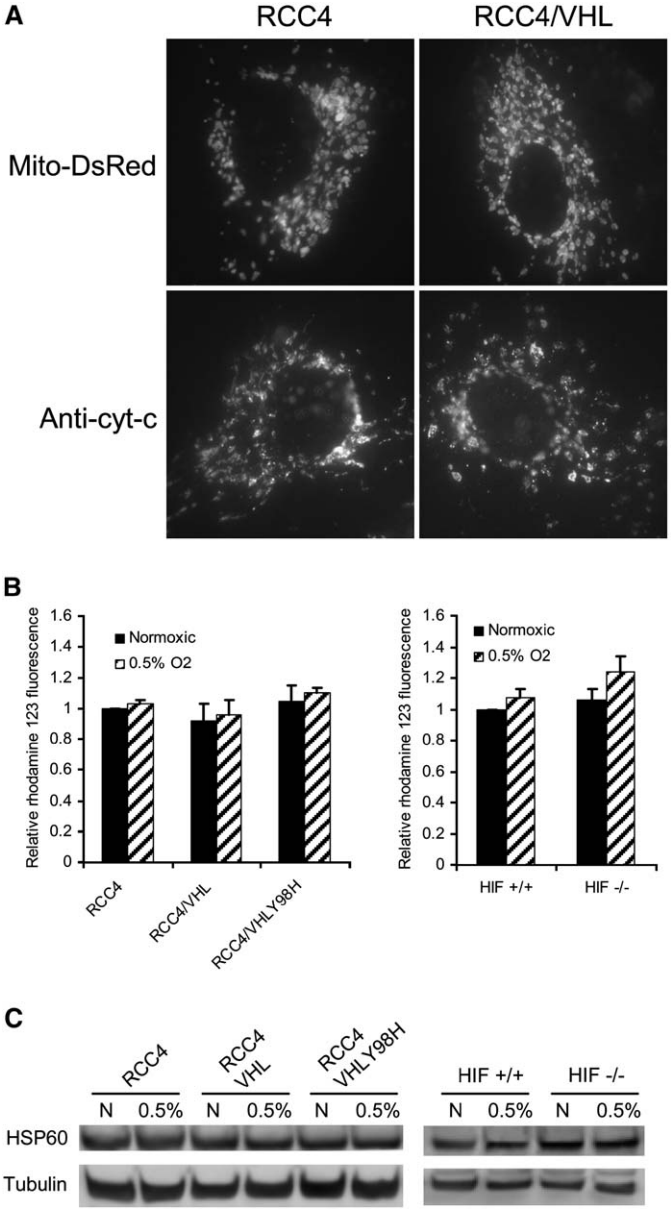

Figure 3. Mitochondria are not grossly altered by hypoxia or HIF activity

A) Fluorescent microscopy of RCC4 and RCC4/VHL cells under normoxic conditions shows no morphologic difference in mitochondria. In the top panels, cells were transiently transfected with mito-DsRed to label mitochondria and visualized with 594 nm excitation. In the bottom panels, immunofluorescence was used to visualize the endogenous mitochondrial protein cytochrome c and detected with anti-mouse Alexa 488 secondary antibody.
B) Mitochondrial membrane potential is not altered in RCC4, RCC4/VHL, RCC4/VHLY98H, HIF wt MEFs, and HIF KO MEFs after exposure to normoxia or 0.5% O_2 for 24 hr. Rhodamine 123 staining and flow cytometry was used to measure the mean fluorescence intensity, which is expressed relative to parental cells under normoxic conditions.
C) Western blot of lysates from the indicated cells exposed to normoxia or 0.5% O_2 for 24 hr were probed for mitochondrial HSP60, a constitutive mitochondrial protein, as a measure of total mitochondrial mass. Blots were reprobed for tubulin as a loading control.
For all graphs, the error bars represent the standard error of the mean.

both induced by hypoxia in a VHL-dependent manner, with the expression of PDK1 inversely matching the oxygen consumption measured in Figure 1 above. Likewise, the HIF wt MEFs show oxygen-dependent induction of PDK1 and BNip3, while the HIF KO MEFs did not show any expression of either of these proteins under any oxygen conditions (Figure 4B). Finally, the parental RKO cells were able to induce PDK1 and the HIF target gene BNip3L in response to hypoxia, while the HIF-depleted ShRNA RKO cells could not induce either protein (Figure 4C). Therefore, in all three cell types, the HIF-1-dependent regulation of oxygen consumption seen in Figure 2, corresponds to the HIF-1-dependent induction of PDK1 seen in Figure 4.

In order to determine if PDK1 was a direct HIF-1 target gene, we analyzed the genomic sequence flanking the 5′ end of the gene for possible HIF-1 binding sites based on the consensus core HRE element (A/G)CGTG (Caro, 2001). Several such sites exist within the first 400 bases upstream, so we generated reporter constructs by fusing the genomic sequence from −400 to +30 of the start site of transcription to the firefly luciferase gene. In transfection experiments, the chimeric construct showed significant induction by either cotransfection with a constitutively active HIF proline mutant (P402A/P564G) (Chan et al., 2002) or exposure of the transfected cells to 0.5% oxygen (Figure 4D). Most noteworthy, when the reporter gene was transfected into the HIF-1α null cells, it did not show induction when the cells were cultured in hypoxia, but it did show induction when cotransfected with expression HIF-1α plasmid. We then generated deletions down to the first 36 bases upstream

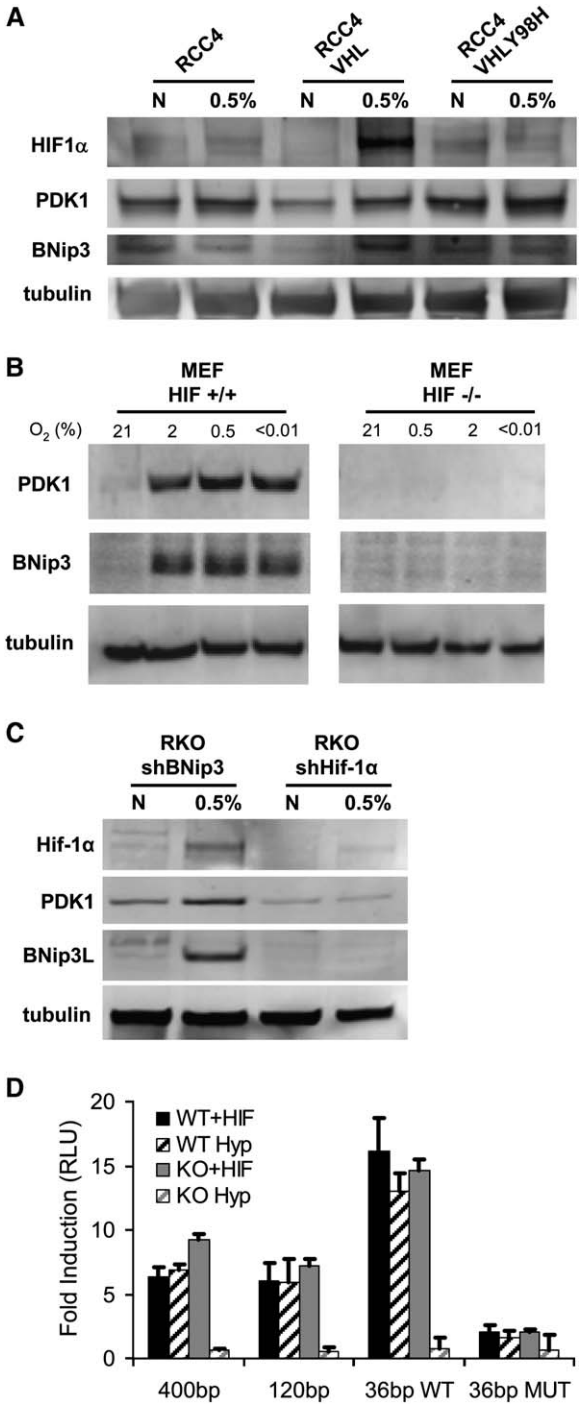

Figure 4. PDK1 protein is upregulated by hypoxia in a HIF-dependent manner

A) Western blots of RCC4, RCC4/VHL, and RCC4/VHLY98H lysates after exposure to normoxia or 0.5% O_2 for 24 hr. Blots were probed for HIF 1α, PDK1, the HIF target gene BNip3, and tubulin as a loading control.

B) Western blots of HIF wt and HIF KO MEF lysates after exposure to the indicated oxygen concentrations for 24 hr. Blots were probed for PDK1, the HIF target gene BNip3, and tubulin as a loading control.

C) Western blots of ShRNABNip3RKO and ShRNAHIF-1αRKO lysates after exposure to normoxia or 0.5% O_2 for 24 hr. Blots were probed for HIF 1α, to demonstrate specific inhibition in the ShHIF 1α cell line, PDK1, the HIF target gene BNip3L, and tubulin as a loading control. Note that BNip3 is not expressed in RKO cells.

D) Analysis of the PDK1 promoter for functional HREs. Segments of DNA taken from the indicated 5′-flanking region were fused to the firefly luciferase gene and transiently transfected into the wild-type and the HIF1α knockout cells as indicated. Cells were either cotransfected with 50 ng of empty vector or HIF1α (P402A/P564G) expression plasmid, or they were treated with 24 hr 0.5% hypoxia as indicated. The relative luciferase activity was measured in a Beckton Dickenson Monolite 2000 and normalized for transfection efficiency using cotransfected renilla luciferase and empty pGL3 for a noninducible construct. The baseline expression of the reporter genes is within 2-fold when comparing normoxic HIF wt to HIF KO cells. Note the loss of HIF-dependent induction in the −36 to +30 fragment when the target HRE is mutated.

For all graphs, the error bars represent the standard error of the mean.

of transcription and found that even this short sequence was responsive to HIF-1 (Figure 4D). Analysis of this small fragment showed only one consensus HRE site located in an inverted orientation in the 5′ untranslated region. We synthesized and cloned a mutant promoter fragment in which the core element ACGTG was replaced with AAAAG, and this construct lost over 90% of its hypoxic induction. These experiments suggest that it is this HRE within the proximal 5′ UTR that HIF-1 uses to transactivate the endogenous PDK1 gene in response to hypoxia.

PDK1 is responsible for the HIF-dependent mitochondrial oxygen consumption changes

In order to directly test if PDK1 was the HIF-1 target gene responsible for the hypoxic reduction in mitochondrial oxygen consumption, we generated RKO cell lines with either knockdown or overexpression of PDK1 and measured the oxygen consumption in these derivatives. The PDK1 ShRNA stable knockdown line was generated as a pool of clones cotransfected with pSUPER ShPDK1 and pTK-hygro resistance gene. After selection for growth in hygromycin, the cells were tested by Western blot for the level of PDK1 protein expression. We found that normoxic PDK1 is reduced by 75%, however, there was measurable expression of PDK1 in these cells in response to hypoxia (Figure 5A). When we measured the corresponding oxygen consumption in these cells, we found a change commensurate with the level of PDK1. The knockdown cells show elevated baseline oxygen consumption, and partial reduction in this activity in response to hypoxia. Therefore, reduction of PDK1 expression by genetic means increased mitochondrial oxygen consumption in both normoxic and hypoxic conditions. Interestingly, these cells still induced HIF-1α (Figure 5A) and HIF-1 target genes such as BNip3L in response to hypoxia (data not shown), suggesting that altered PDK1 levels do not alter HIF-1α function.

We also determined if overexpression of PDK1 could lead to reduced mitochondrial oxygen consumption. A separate culture of RKO cells was transfected with a PDK1-IRES-puro expression plasmid and selected for resistance to puromycin. The pool of puromycin resistant cells was tested for PDK1 expression by Western blot. These cells showed a modest increase in PDK1 expression under control conditions when compared to the cells transfected with GUS-IRES-puro, with an additional increase in PDK1 protein in response to hypoxia (Figure 5C). The corresponding oxygen consumption measurements showed that the mitochondria is very sensitive to changes in the levels of PDK1, as even this slight increase was able to significantly reduce oxygen consumption in the normoxic PDK1-puro cultures. Further increase in PDK1 levels with hypoxia further reduced oxygen consumption in both cultures (Figure 5D). The model describing the relationship between hypoxia, HIF-1, PDK1, and intermediate metabolism is described in Figure 5E.

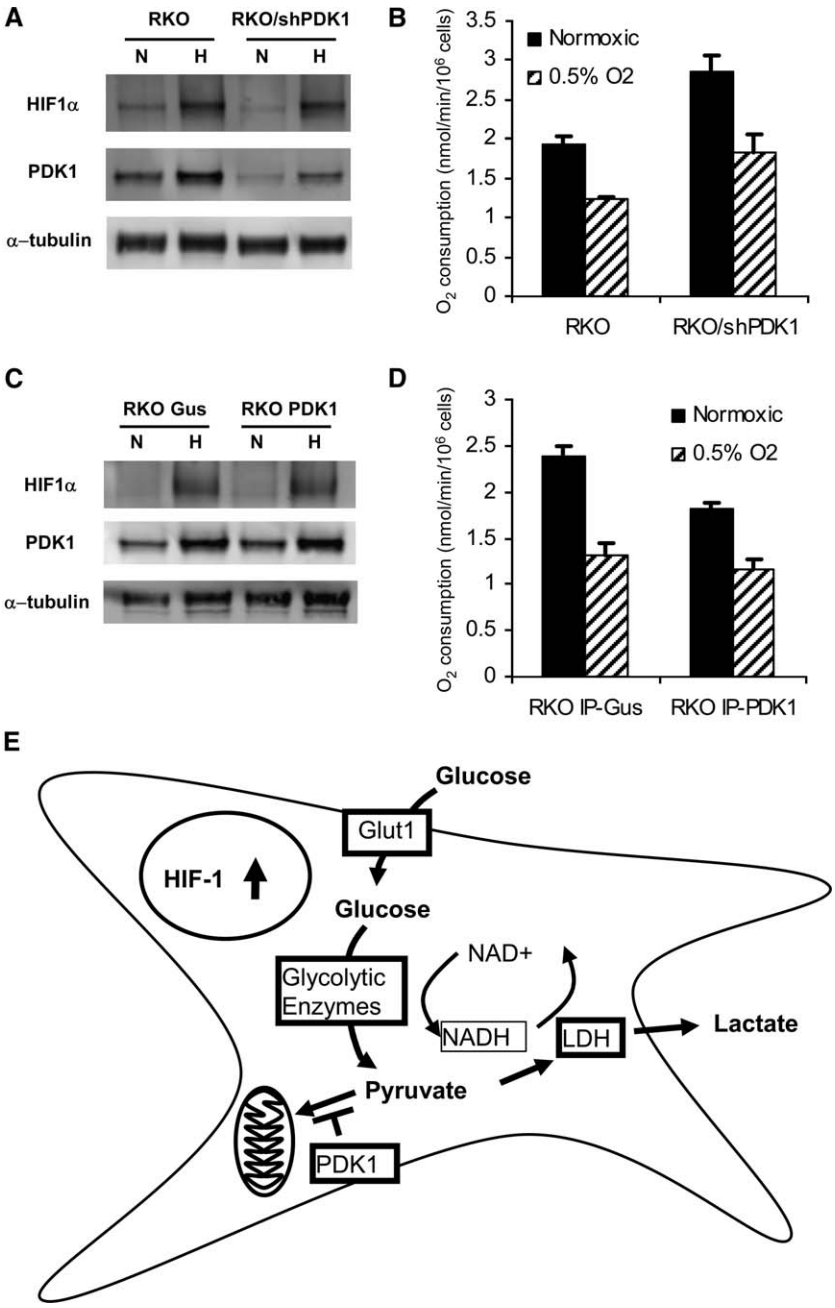

Figure 5. PDK1 expression directly regulates cellular oxygen consumption rate

A) Western blot of RKO cell and ShRNAPDK1RKO cell lysates after exposure to 24 hr of normoxia or 0.5% O_2. Blots were probed for HIF 1α, PDK1, and tubulin as a loading control.

B) Oxygen consumption rate in RKO and ShRNAPDK1RKO cells after exposure to 24 hr of normoxia or 0.5% O_2.

C) Western blot of RKOiresGUS cell and RKOiresPDK1 cell lysates after exposure to 24 hr of normoxia or 0.5% O_2. Blots were probed for HIF 1α, PDK1, and tubulin as a loading control.

D) Oxygen consumption rate in RKOiresGUS and RKOiresPDK1 cells after exposure to 24 hr of normoxia or 0.5% O_2.

E) Model describing the interconnected effects of HIF-1 target gene activation on hypoxic cell metabolism. Reduced oxygen conditions causes HIF-1 to coordinately induce the enzymes shown in boxes. HIF-1 activation results in increased glucose transporter expression to increase intracellular glucose flux, induction of glycolytic enzymes increases the conversion of glucose to pyruvate generating energy and NADH, induction of PDK1 decreases mitochondrial utilization of pyruvate and oxygen, and induction of LDH increases the removal of excess pyruvate as lactate and also regenerates NAD+ for increased glycolysis.

For all graphs, the error bars represent the standard error of the mean.

Altering oxygen consumption alters intracellular oxygen tension and sensitivity to hypoxia-dependent cell killing

The intracellular concentration of oxygen is a net result of the rate at which oxygen diffuses into the cell and the rate at which it is consumed. We hypothesized that the rate at which oxygen was consumed within the cell would significantly affect its steady-state intracellular concentrations. We tested this hypothesis in vitro using the hypoxic marker drug pimonidazole (Bennewith and Durand, 2004). We plated high density cultures of HIF wild-type and HIF knockout cells and placed these cultures in normoxic, 2% oxygen, and anoxic incubators for overnight treatment. The overnight treatment gives the cells time to adapt to the hypoxic conditions and establish altered oxygen consumption profiles. Pimonidozole was then added for the last 4 hr of the growth of the culture. Pimonidazole binding was detected after fixation of the cells using an FITC labeled anti-pimonidazole antibody and it was quantitated by flow cytometry. The quantity of the bound drug is a direct indication of the oxygen concentration within the cell (Bennewith and Durand, 2004). The histograms in Figure 6A show that the HIF-1 knockout and wild-type cells show similar staining in the cells grown in 0% oxygen. However, the cells treated with 2% oxygen show the consequence of the genetic removal of HIF-1. The HIF-proficient cells showed relatively less pimonidazole binding at 2% when compared to the 0% culture, while the HIF-deficient cells showed identical binding between the cells at 2% and those at 0%. We interpret these results to mean that the HIF-deficient cells have greater oxygen consumption, and this has lowered the intracellular oxygenation from the ambient 2% to close to zero intracellularly. The HIF-proficient cells reduced their

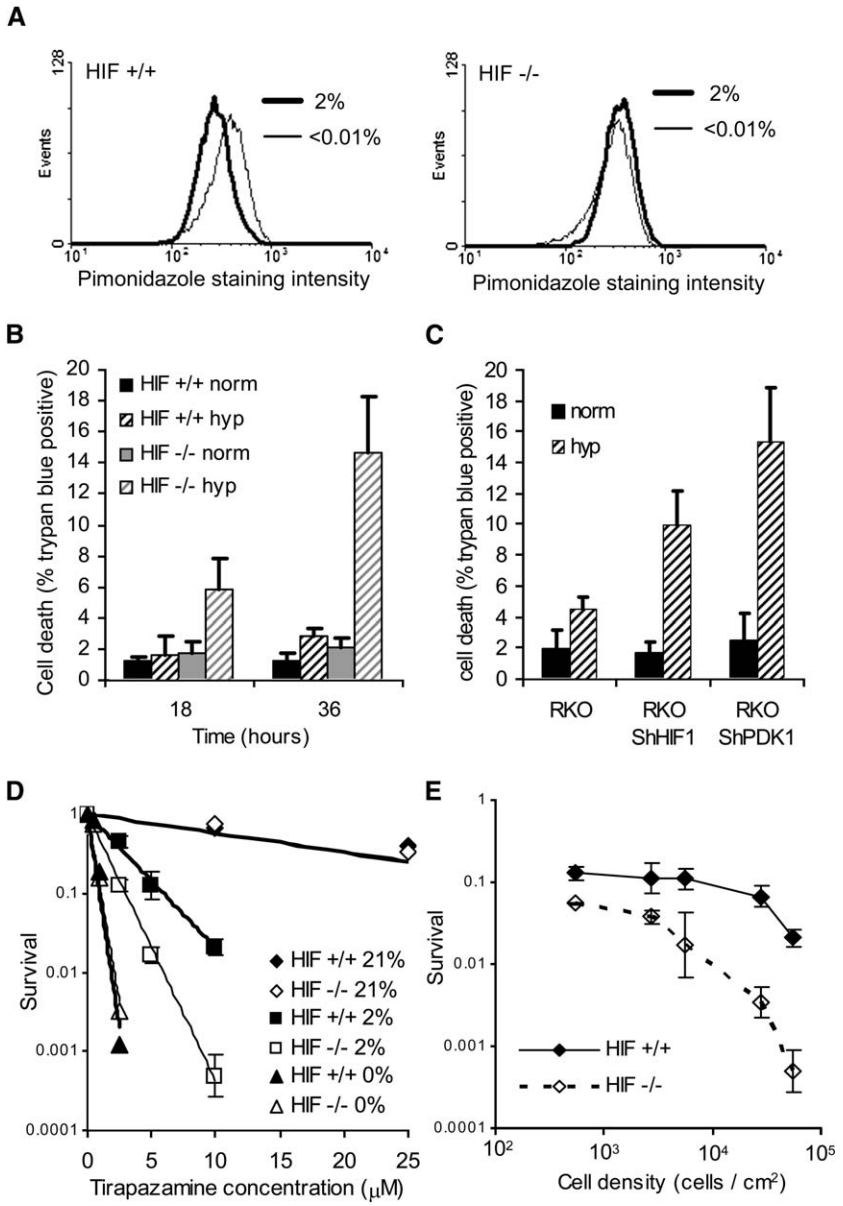

Figure 6. HIF-dependent decrease in oxygen consumption raises intracellular oxygen concentration, protects when oxygen is limiting, and decreases sensitivity to tirapazamine in vitro

A) Pimonidazole was used to determine the intracellular oxygen concentration of cells in culture. HIF wt and HIF KO MEFs were grown at high density and exposed to 2% O_2 or anoxia for 24 hr in glass dishes. For the last 4 hr of treatment, cells were exposed to 60 μg/ml pimonidazole. Pimonidazole binding was quantitated by flow cytometry after binding of an FITC conjugated anti-pimo mAb. Results are representative of two independent experiments.

B) HIF1α reduces oxygen consumption and protects cells when total oxygen is limited. HIF wt and HIF KO cells were plated at high density and sealed in aluminum jigs at <0.02% oxygen. At the indicated times, cells were harvested, and dead cells were quantitated by trypan blue exclusion. Note both cell lines are equally sensitive to anoxia-induced apoptosis, so the death of the HIF null cells indicates that the increased oxygen consumption removed any residual oxygen in the jig and resulted in anoxia-induced death.

C) PDK1 is responsible for HIF-1's adaptive response when oxygen is limiting. A similar jig experiment was performed to measure survival in the parental RKO, the RKO ShRNAHIF1α, and the RKOShPDK1 cells. Cell death by trypan blue uptake was measured 48 hr after the jigs were sealed.

D) HIF status alters sensitivity to TPZ in vitro. HIF wt and HIF KO MEFs were grown at high density in glass dishes and exposed to 21%, 2%, and <0.01% O_2 conditions for 18 hr in the presence of varying concentrations of Tirapazamine. After exposure, cells were harvested and replated under normoxia to determine clonogenic viability. Survival is calculated relative to the plating efficiency of cells exposed to 0 μM TPZ for each oxygen concentration.

E) Cell density alters sensitivity to TPZ. HIF wt and HIF KO MEFs were grown at varying cell densities in glass dishes and exposed to 2% O_2 in the presence of 10 μM TPZ for 18 hr. After the exposure, survival was determined as described in (**C**).

For all graphs, the error bars represent the standard error of the mean.

oxygen consumption rate so that the rate of diffusion into the cell is greater than the rate of consumption.

HIF-induced PDK1 can reduce the total amount of oxygen consumed per cell. The reduction in the amount of oxygen consumed could be significant if there is a finite amount of oxygen available, as would be the case in the hours following a blood vessel occlusion. The tissue that is fed by the vessel would benefit from being economical with the oxygen that is present. We experimentally modeled such an event using aluminum jigs that could be sealed with defined amounts of cells and oxygen present (Siim et al., 1996). We placed 10×10^6 wild-type or HIF null cells in the sealed jig at 0.02% oxygen, waited for the cells to consume the remaining oxygen, and measured cell viability. We have previously shown that these two cell types are resistant to mild hypoxia and equally sensitive to anoxia-induced apoptosis (Papandreou et al., 2005a). Therefore, any death in this experiment would be the result of the cells consuming the small amount of remaining oxygen and dying in response to anoxia. We found that in sealed jigs, the wild-type cells are more able to adapt to the limited oxygen supply by reducing consumption. The HIF null cells continued to consume oxygen, reached anoxic levels, and started to lose viability within 36 hr (Figure 6B). This is a secondary adaptive effect of HIF1. We confirmed that PDK1 was responsible for this difference by performing a similar experiment using the parental RKO cells, the RKOShRNAHIF1α and the RKOShRNAPDK1 cells. We found similar results in which both the cells with HIF1α knockdown and PDK1 knockdown were sensitive to the long-term effects of being sealed in a jig with a defined amount of oxygen (Figure 6c). Note that the RKOShPDK1 cells are even more sensitive than the RKOShHIF1α cells, presumably because they have higher basal oxygen consumption rates (Figure 5B).

Because HIF-1 can help cells adapt to hypoxia and maintain some intracellular oxygen level, it may also protect tumor cells from killing by the hypoxic cytotoxin tirapazamine (TPZ). TPZ toxicity is very oxygen dependent, especially at oxygen levels

between 1%–4% (Koch, 1993). We therefore tested the relative sensitivity of the HIF wt and HIF KO cells to TPZ killing in high density cultures (Figure 6D). We exposed the cells to the indicated concentrations of drug and oxygen concentrations overnight. The cells were then harvested and replated to determine reproductive viability by colony formation. Both cell types were equally resistant to TPZ at 21% oxygen, while both cell types are equally sensitive to TPZ in anoxic conditions where intracellular oxygen levels are equivalent (Figure 6A). The identical sensitivity of both cell types in anoxia indicates that both cell types are equally competent in repairing the TPZ-induced DNA damage that is presumed to be responsible for its toxicity. However, in 2% oxygen cultures, the HIF null cells displayed a significantly greater sensitivity to the drug than the wild-type cells. This suggests that the increased oxygen consumption rate in the HIF-deficient cells is sufficient to lower the intracellular oxygen concentration relative to that in the HIF-proficient cells. The lower oxygen level is significant enough to dramatically sensitize these cells to killing by TPZ.

If the increased sensitivity to TPZ in the HIF ko cells is determined by intracellular oxygen consumption differences, then this effect should also be cell-density dependent. We showed that this is indeed the case in Figure 6E where oxygen and TPZ concentrations were held constant, and increased cell density lead to increased TPZ toxicity. The effect was much more pronounced in the HIF KO cells, although the HIF wt cells showed some increased toxicity in the highest density cultures, consistent with the fact they were still consuming some oxygen, even with HIF present (Figure 1). The in vitro TPZ survival data is therefore consistent with our hypothesis that control of oxygen consumption can regulate intracellular oxygen concentration, and suggests that increased oxygen consumption could sensitize cells to hypoxia-dependent therapy.

Discussion

The findings presented here show that HIF-1 is actively responsible for regulating energy production in hypoxic cells by an additional, previously unrecognized mechanism. It has been shown that HIF-1 induces the enzymes responsible for glycolysis when it was presumed that low oxygen did not support efficient oxidative phosphorylation (Iyer et al., 1998; Seagroves et al., 2001). The use of glucose to generate ATP is capable of satisfying the energy requirements of a cell if glucose is in excess (Papandreou et al., 2005a). We now find that at the same time that glycolysis is increasing, mitochondrial respiration is decreasing. However, the decreased respiration is not because there is not enough oxygen present to act as a substrate for oxidative phosphorylation, but because the flow of pyruvate into the TCA cycle has been reduced by the activity of pyruvate dehydrogenase kinase. Other reports have suggested that oxygen utilization is shifted in cells exposed to hypoxia, but these reports have focused on other regulators such as nitric oxide synthase (Hagen et al., 2003). NO can reduce oxygen consumption through direct inhibition of cytochrome oxidase, but this effect seems to be more significant at physiologic oxygen concentrations, not at severe levels seen in the tumor (Palacios-Callender et al., 2004).

Several reports have also suggested a link between altered mitochondrial function in hypoxia and HIF activation (Brunelle et al., 2005; Guzy et al., 2005; Mansfield et al., 2005). While the models are not mutually exclusive, our results indicate that HIF target gene activation is upstream of mitochondrial function, and responsible for altering mitochondrial activity. The question becomes more complicated with the acute (biochemical) and chronic (epigenetic) changes that occur with different kinetics. In fact, there may be several levels of adaptive response and feedback-feedforward cycles such as the recently reported downregulation of succinate dehydrogenase by hypoxia (Dahia et al., 2005).

This hypoxic shift in intermediate metabolism away from oxidative phosphorylation provides an elegant means for the cell to maintain both energy and redox states (diagrammed in Figure 5) (Semenza et al., 2001). ATP is produced through the breakdown of glucose to pyruvate but requires NAD as a cofactor for glyceraldehyde phosphate dehydrogenase (GAPDH), where it is reduced into NADH. NADH is routinely oxidized by the mitochondria to produce high energy electrons for electron chain transfer and is regenerated to NAD for glycolysis. Under anoxic conditions, NADH is not recycled by the mitochondria, and so it must be regenerated by another means. The alternative nonoxygen requiring pathway is through the conversion of pyruvate to lactate by lactate dehydrogenase (LDH). Lactate is secreted into the extracellular space, and NAD is regenerated. The NAD cycle and redox state of the cell is therefore maintained through the activity of several interrelated systems, all of which are coordinately regulated by HIF-1 (glycolytic enzymes, pyruvate dehydrogenase kinase, and lactate dehydrogenase) (Leong et al., 2003).

Inhibiting HIF-1 activity in the hypoxic tumor cells is predicted to have several therapeutic effects. One primary rationale for targeting HIF-1 is that it should only be activated within the hypoxic tumor, so that therapy directed against HIF should not have systemic side effects. Current tumor models suggest that inhibiting HIF target genes such as VEGF will reduce tumor angiogenesis (Moeller et al., 2004). However, the data supporting HIF inhibition as a means for direct tumor toxicity are mixed, and it appears that a HIF inhibitor will probably not be curative on its own. It is therefore imperative to determine what would be the most effective combination of drugs to use with a HIF inhibitor. We propose that one result of HIF inhibition would be to increase oxygen consumption and make tumors more hypoxic. HIF inhibitors might therefore be best used in clinical practice in conjunction with hypoxic cytotoxins such as Tirapazamine.

Experimental procedures

Cell lines and cell culture

Primary human fibroblasts have been described (Denko et al., 2003) and RKO human colon carcinoma cells were obtained from the American Type Culture Collection (ATCC, Manassas, VA). RCC4, RCC4/VHL, and RCC4/Y98H human renal cell carcinoma cell lines have also been described previously (Chan et al., 2005). Wild-type and HIF-1α knockout mouse embryo fibroblasts (MEFs) were a gift from Dr. R Johnson (University of California, San Diego). All cells were grown in Dulbecco's Modified Eagle's Media (DMEM) supplemented with 10% fetal bovine serum (FBS). For moderate hypoxia, cell culture dishes were placed into an Invivo$_2$ humidified hypoxia workstation (Ruskinn Technologies, Bridgend, UK) at the indicated oxygen concentrations. Severe hypoxia was generated in an anaerobic workstation with a palladium catalyst (Sheldon Co., Cornelius, OR). Tirapazamine (a gift of M. Brown, Stanford University) toxicity was measured in cells after overnight growth at the indicated density in glass dishes. The next day, fresh media was added containing the indicated concentration of TPZ, and the cells

placed in the indicated oxygen environment. Eighteen hours later, the cells were trypsinized, counted, and plated for colony formation in normoxia.

Plasmids and siRNAs

Full-length human PDK1 cDNA was obtained from the mammalian gene collection (MGC), through the ATCC, and was cloned into pEF2aIRESpuro creating pPDK1IRESpuro. pDsRed2-mito was constructed by cloning a 28 amino acid mitochondrial targeting sequence from human cytochrome c oxidase subunit VIII into the pDsRed2-N1 vector (Clontech, Mountain View, CA). For knockdown experiments, the target sequences used were: HIF-1α, UGAGGAAGUACCAUUAUAU and PDK1, CGACACAAUGAUGUCAU UCCCACAA. For construction of stable knockdown cell lines, the sequences listed above were cloned into pSUPER using synthetic 64-mer oligonucleotides (Brummelkamp et al., 2002). RKO/shPDK1 and RKO/shHIF-1α stable knockdown cells were created by cotransfecting RKO cells with pTKhygro, and either empty pSuper, pSuper-shPDK1 or pSuper-shHIF-1α (1:20 ratio) using Lipofectamine (Invitrogen, Carlsbad, CA), followed by selection in 500 ug/ml hygromycin. The RKOPDK1IRESpuro stable overexpressing cell lines were established by transfecting RKO cells with pPDK1IRESpuro using Lipofectamine followed by culture in 2 μg/ml puromycin.

Microarray analysis

Total RNA was extracted using TriZol reagent (Invitrogen). Preparation of cDNA and cRNA was conducted following instructions in the Affymetrix GeneChip Expression Analysis Manual (Affymetrix, Santa Clara, CA). cRNA was hybridized to an oligo-based array, washed and scanned according to standard Affymetrix protocols. Data from the scanning of the Affymetrix GeneChips was gathered using the Affymetrix Microarray Suite v4.0 and exported to Microsoft Excel.

Oxygen consumption measurements

Cells were trypsinized and suspended at 3×10^6 to 6×10^6 cells per ml in normoxic DMEM + 10% FBS. Oxygen consumption was measured in a 0.5 ml volume using an Oxytherm electrode unit (Hansatech, Norfolk, UK). This system employs a Clark-type oxygen electrode to monitor the dissolved oxygen concentration in a sealed measurement chamber over time. The data are exported to a computerized chart recorder (Oxygraph 1.01, Hansatech, Norfolk, UK), which calculates the rate of oxygen consumption. A small stir bar maintains the cells in suspension, and a peltier heating block maintains the temperature at 37ºC. Since the electrode consumes oxygen during measurement, the rate of oxygen drop in 0.5 ml of DMEM media without cells was established and subtracted from the total oxygen consumption rates for the cell suspensions.

Western blotting

In brief, treated cells were harvested directly in RIPA buffer containing protease inhibitors, protein concentrations were quantitated, 25–50 μg were electrophoresed on a reducing Tris-Tricine gel, and electroblotted to PVDF membrane. Antibodies used were murine α-HIF-1 Transduction Labs (1:1000), rabbit α-PDK1 Stressgen (1:2000), murine α-α tubulin Research Diagnostics (1:2000) goat α-HSP60 Santa Cruz (1:2000), and rabbit α-Bnip3 and α Bnip3L were described previously (1:500) (Papandreou et al., 2005a). Primary antibodies were detected with species-specific secondary antibodies labeled with Alkaline Phosphatase (Vector labs 1:3000) and visualized with ECF (Amersham) on a Storm 860 phosphoimager (Molecular Devices).

Mitochondrial membrane potential staining and flow cytometry

Rhodamine 123 (R123) (Molecular Probes, Eugene, OR) uptake was used to measure mitochondrial membrane potential. Cells were trypsinized, counted, and suspended at 5×10^5 cells per ml in DMEM + 10% FBS with 10 μg/ml R123, at 37ºC for 10 min. The cells were pelleted by centrifugation and resuspended in cold DMEM + 10% FBS. Fluorescence was measured in a FACSCalibur flow cytometer (Becton Dickinson, San Jose, CA). Forward scatter and side scatter values were used to gate on whole cells, and R123 fluorescence was measured for 10,000 cells per sample using the FL2 channel. All gain and amplifier settings were held constant for the duration of the experiment. Since the R123 fluorescence values for all samples displayed a log normal distribution, the geometric mean was used as a quantitative measure of the cell population's membrane potential.

Immunocytochemistry and fluorescence microscopy

Cells were plated on glass multiwell chamber slides (Nalge Nunc, Naperville, IL) in DMEM + 10% FBS. For examination of mitochondrial DsRed2, cells were transfected using Lipofectamine, 48 hr later they were fixed in 4% paraformaldehyde, and mounted in Vectashield (Vector Laboratories, Burlingame, CA). For cytochrome c immunocytochemistry, chamber slides were fixed in 4% paraformaldehyde, blocked in PBS Tween milk (0.2% Tween 20, 5% nonfat dry milk, in PBS) overnight at 4 C. Cytochrome c was visualized using a mouse monoclonal antibody 1:250 (BD Pharmingen, San Diego, CA) and an anti-mouse Alexa 488 secondary antibody 1:500 (Molecular Probes). Cells were visualized on a Nikon Eclipse E800 microscope, with a Spot RT Slider CCD digital camera using standard FITC and Texas Red filter blocks (Diagnostic Instruments, Sterling Heights, MI).

Pimonidazole staining

Hypoxyprobe 1 (pimonidazole hydrochloride) was purchased from Chemicon (Temecula, CA). Cells were treated at 60 mg/liter in the culture medium during the final 4 hr of the hypoxic exposure, harvested, fixed in 4% paraformaldehyde, blocked in PBS containing 5% nonfat dry milk and 0.1%Triton and 4% FBS (PBS-T-milk-FBS). After 2 hr blocking, cells were treated with FITC-labeled anti-pimonidozole mAb at 1:25 dilution for 2 hr in PBS-T-milk-FBS. The cells were then washed in PBS-T-milk-FBS and relative FITC was measured on FL1 in a Beckton-Dickenson FacScanner.

Data analysis

Oxygen consumption experiments were repeated three times in duplicate, survival was measured three times in triplicate, reporter assays were repeated two times in quadruplicate. Error bars represent the standard error of the mean.

Supplemental data

Supplemental data include one table and can be found with this article online at http://www.cellmetabolism.org/cgi/content/full/3/3/187/DC1/.

Acknowledgments

This work was supported by grant CA67166 from the National Cancer Institute (NCI). These findings were first presented at the NCI Workshop "Mitochondrial Function and Cancer" in May 2004 (Perry et al., 2004).

Received: November 3, 2005
Revised: December 19, 2005
Accepted: January 31, 2006
Published: March 7, 2006

References

Airley, R., Loncaster, J., Davidson, S., Bromley, M., Roberts, S., Patterson, A., Hunter, R., Stratford, I., and West, C. (2001). Glucose transporter glut-1 expression correlates with tumor hypoxia and predicts metastasis-free survival in advanced carcinoma of the cervix. Clin. Cancer Res. *7*, 928–934.

Bennewith, K.L., and Durand, R.E. (2004). Quantifying transient hypoxia in human tumor xenografts by flow cytometry. Cancer Res. *64*, 6183–6189.

Brizel, D.M., Scully, S.P., Harrelson, J.M., Layfield, L.J., Bean, J.M., Prosnitz, L.R., and Dewhirst, M.W. (1996). Tumor oxygenation predicts for the likelihood of distant metastases in human soft tissue sarcoma. Cancer Res. *56*, 941–943.

Brown, G.C. (1992). Control of respiration and ATP synthesis in mammalian mitochondria and cells. Biochem. J. *284*, 1–13.

Brown, J.M., and Giaccia, A.J. (1998). The unique physiology of solid tumors: opportunities (and problems) for cancer therapy. Cancer Res. *58*, 1408–1416.

Bruick, R.K., and McKnight, S.L. (2001). A conserved family of prolyl-4-hydroxylases that modify HIF. Science *294*, 1337–1340.

Brummelkamp, T.R., Bernards, R., and Agami, R. (2002). A system for stable expression of short interfering RNAs in mammalian cells. Science *296*, 550–553.

Brunelle, J.K., Bell, E.L., Quesada, N.M., Vercauteren, K., Tiranti, V., Zeviani, M., Scarpulla, R.C., and Chandel, N.S. (2005). Oxygen sensing requires mitochondrial ROS but not oxidative phosphorylation. Cell Metab *1*, 409–414.

Cairns, R.A., and Hill, R.P. (2004). Acute hypoxia enhances spontaneous lymph node metastasis in an orthotopic murine model of human cervical carcinoma. Cancer Res. *64*, 2054–2061.

Caro, J. (2001). Hypoxia regulation of gene transcription. High Alt. Med. Biol. *2*, 145–154.

Chan, D.A., Sutphin, P.D., Denko, N.C., and Giaccia, A.J. (2002). Role of prolyl hydroxylation in oncogenically stabilized hypoxia-inducible factor-1alpha. J. Biol. Chem. *277*, 40112–40117.

Chan, D.A., Sutphin, P.D., Yen, S.E., and Giaccia, A.J. (2005). Coordinate regulation of the oxygen-dependent degradation domains of hypoxia-inducible factor 1(alpha). Mol. Cell. Biol. *25*, 6415–6426.

Chandel, N.S., Budinger, G.R., Choe, S.H., and Schumacker, P.T. (1997). Cellular respiration during hypoxia. Role of cytochrome oxidase as the oxygen sensor in hepatocytes. J. Biol. Chem. *272*, 18808–18816.

Dahia, P.L., Ross, K.N., Wright, M.E., Hayashida, C.Y., Santagata, S., Barontini, M., Kung, A.L., Sanso, G., Powers, J.F., Tischler, A.S., et al. (2005). A HIF1alpha regulatory loop links hypoxia and mitochondrial signals in pheochromocytomas. PLoS Genet *1*, 72–80.

Denko, N.C., Fontana, L.A., Hudson, K.M., Sutphin, P.D., Raychaudhuri, S., Altman, R., and Giaccia, A.J. (2003). Investigating hypoxic tumor physiology through gene expression patterns. Oncogene *22*, 5907–5914.

Epstein, A.C., Gleadle, J.M., McNeill, L.A., Hewitson, K.S., O'Rourke, J., Mole, D.R., Mukherji, M., Metzen, E., Wilson, M.I., Dhanda, A., et al. (2001). C. elegans EGL-9 and mammalian homologs define a family of dioxygenases that regulate HIF by prolyl hydroxylation. Cell *107*, 43–54.

Graeber, T.G., Osmanian, C., Jacks, T., Housman, D.E., Koch, C.J., Lowe, S.W., and Giaccia, A.J. (1996). Hypoxia-mediated selection of cells with diminished apoptotic potential in solid tumours. Nature *379*, 88–91.

Greijer, A.E., van der Groep, P., Kemming, D., Shvarts, A., Semenza, G.L., Meijer, G.A., van de Wiel, M.A., Belien, J.A., van Diest, P.J., and van der Wall, E. (2005). Up-regulation of gene expression by hypoxia is mediated predominantly by hypoxia-inducible factor 1 (HIF-1). J. Pathol. *206*, 291–304.

Gulledge, C.J., and Dewhirst, M.W. (1996). Tumor oxygenation: a matter of supply and demand. Anticancer Res. *16*, 741–749.

Guzy, R.D., Hoyos, B., Robin, E., Chen, H., Liu, L., Mansfield, K.D., Simon, M.C., Hammerling, U., and Schumacker, P.T. (2005). Mitochondrial complex III is required for hypoxia-induced ROS production and cellular oxygen sensing. Cell Metab *1*, 401–408.

Hagen, T., Taylor, C.T., Lam, F., and Moncada, S. (2003). Redistribution of intracellular oxygen in hypoxia by nitric oxide: effect on HIF1alpha. Science *302*, 1975–1978.

Hockel, M., Schlenger, K., Aral, B., Mitze, M., Schaffer, U., and Vaupel, P. (1996). Association between tumor hypoxia and malignant progression in advanced cancer of the uterine cervix. Cancer Res. *56*, 4509–4515.

Hockel, M., and Vaupel, P. (2001). Tumor hypoxia: definitions and current clinical, biologic, and molecular aspects. J. Natl. Cancer Inst. *93*, 266–276.

Holness, M.J., and Sugden, M.C. (2003). Regulation of pyruvate dehydrogenase complex activity by reversible phosphorylation. Biochem. Soc. Trans. *31*, 1143–1151.

Ivan, M., Kondo, K., Yang, H., Kim, W., Valiando, J., Ohh, M., Salic, A., Asara, J.M., Lane, W.S., and Kaelin, W.G., Jr. (2001). HIFalpha targeted for VHL-mediated destruction by proline hydroxylation: implications for O2 sensing. Science *292*, 464–468.

Iyer, N.V., Kotch, L.E., Agani, F., Leung, S.W., Laughner, E., Wenger, R.H., Gassmann, M., Gearhart, J.D., Lawler, A.M., Yu, A.Y., and Semenza, G.L. (1998). Cellular and developmental control of O2 homeostasis by hypoxia-inducible factor 1 alpha. Genes Dev. *12*, 149–162.

Jaakkola, P., Mole, D.R., Tian, Y.M., Wilson, M.I., Gielbert, J., Gaskell, S.J., Kriegsheim, A., Hebestreit, H.F., Mukherji, M., Schofield, C.J., et al. (2001). Targeting of HIF-alpha to the von Hippel-Lindau ubiquitylation complex by O2-regulated prolyl hydroxylation. Science *292*, 468–472.

Kimura, S., Kitadai, Y., Tanaka, S., Kuwai, T., Hihara, J., Yoshida, K., Toge, T., and Chayama, K. (2004). Expression of hypoxia-inducible factor (HIF)-1alpha is associated with vascular endothelial growth factor expression and tumour angiogenesis in human oesophageal squamous cell carcinoma. Eur. J. Cancer *40*, 1904–1912.

Koch, C.J. (1993). Unusual oxygen concentration dependence of toxicity of SR-4233, a hypoxic cell toxin. Cancer Res. *53*, 3992–3997.

Kondo, K., Kim, W.Y., Lechpammer, M., and Kaelin, W.G., Jr. (2003). Inhibition of HIF2alpha is sufficient to suppress pVHL-defective tumor growth. PLoS Biol. *1*, e83. 10.1371/journal.pbio.0000083.

Koukourakis, M.I., Giatromanolaki, A., Sivridis, E., Gatter, K.C., and Harris, A.L. (2005). Pyruvate dehydrogenase and pyruvate dehydrogenase kinase expression in non small cell lung cancer and tumor-associated stroma. Neoplasia *7*, 1–6.

Leong, H.S., Brownsey, R.W., Kulpa, J.E., and Allard, M.F. (2003). Glycolysis and pyruvate oxidation in cardiac hypertrophy–why so unbalanced? Comp. Biochem. Physiol. A Mol. Integr. Physiol. *135*, 499–513.

Mansfield, K.D., Guzy, R.D., Pan, Y., Young, R.M., Cash, T.P., Schumacker, P.T., and Simon, M.C. (2005). Mitochondrial dysfunction resulting from loss of cytochrome c impairs cellular oxygen sensing and hypoxic HIF-alpha activation. Cell Metab *1*, 393–399.

Maxwell, P.H., Wiesener, M.S., Chang, G.W., Clifford, S.C., Vaux, E.C., Cockman, M.E., Wykoff, C.C., Pugh, C.W., Maher, E.R., and Ratcliffe, P.J. (1999). The tumour suppressor protein VHL targets hypoxia-inducible factors for oxygen-dependent proteolysis. Nature *399*, 271–275.

Moeller, B.J., Cao, Y., Li, C.Y., and Dewhirst, M.W. (2004). Radiation activates HIF-1 to regulate vascular radiosensitivity in tumors: role of reoxygenation, free radicals, and stress granules. Cancer Cell *5*, 429–441.

Nordsmark, M., and Overgaard, J. (2004). Tumor hypoxia is independent of hemoglobin and prognostic for loco-regional tumor control after primary radiotherapy in advanced head and neck cancer. Acta Oncol. *43*, 396–403.

Palacios-Callender, M., Quintero, M., Hollis, V.S., Springett, R.J., and Moncada, S. (2004). Endogenous NO regulates superoxide production at low oxygen concentrations by modifying the redox state of cytochrome c oxidase. Proc. Natl. Acad. Sci. USA *101*, 7630–7635.

Papandreou, I., Krishna, C., Kaper, F., Cai, D., Giaccia, A.J., and Denko, N.C. (2005a). Anoxia is necessary for tumor cell toxicity caused by a low-oxygen environment. Cancer Res. *65*, 3171–3178.

Papandreou, I., Powell, A., Lim, A.L., and Denko, N. (2005b). Cellular reaction to hypoxia: sensing and responding to an adverse environment. Mutat. Res. *569*, 87–100.

Perry, M.E., Dang, C.V., Hockenbery, D., and Moll, U. (2004). Highlights of the National Cancer Institute Workshop on mitochondrial function and cancer. Cancer Res. *64*, 7640–7644.

Roche, T.E., Baker, J.C., Yan, X., Hiromasa, Y., Gong, X., Peng, T., Dong, J., Turkan, A., and Kasten, S.A. (2001). Distinct regulatory properties of pyruvate dehydrogenase kinase and phosphatase isoforms. Prog. Nucleic Acid Res. Mol. Biol. *70*, 33–75.

Seagroves, T.N., Ryan, H.E., Lu, H., Wouters, B.G., Knapp, M., Thibault, P., Laderoute, K., and Johnson, R.S. (2001). Transcription factor HIF-1 is a necessary mediator of the pasteur effect in mammalian cells. Mol. Cell. Biol. *21*, 3436–3444.

Semenza, G.L. (2004). O2-regulated gene expression: transcriptional control of cardiorespiratory physiology by HIF-1. J. Appl. Physiol. *96*, 1173–1177.

Semenza, G.L., Artemov, D., Bedi, A., Bhujwalla, Z., Chiles, K., Feldser, D., Laughner, E., Ravi, R., Simons, J., Taghavi, P., and Zhong, H. (2001). 'The metabolism of tumours': 70 years later. Novartis Found. Symp. *240*, 251–260.

Siim, B.G., van Zijl, P.L., and Brown, J.M. (1996). Tirapazamine-induced DNA damage measured using the comet assay correlates with cytotoxicity towards hypoxic tumour cells in vitro. Br. J. Cancer *73*, 952–960.

Sugden, M.C., and Holness, M.J. (2003). Recent advances in mechanisms regulating glucose oxidation at the level of the pyruvate dehydrogenase complex by PDKs. Am. J. Physiol. Endocrinol. Metab. *284*, E855–E862.

Wang, G.L., and Semenza, G.L. (1993). General involvement of hypoxia-inducible factor 1 in transcriptional response to hypoxia. Proc. Natl. Acad. Sci. USA *90*, 4304–4308.

Accession numbers

Microarray raw data has been uploaded to National Center for Biotechnology Information (NCBI) Gene Expression Omnibus (GEO) database for public access with the accession number GSE4186.